Rare Metal Materials and Engineering
Volume 55, Issue 7, July 2026
Available online at www.rmme.ac.cn

Science Press

Cite this article as: Ji Wei, Zhang Zhaohuang, Lu Zichuan, et al. Wall Thickness Homogenization Control and Performance of Superplastically Formed Hemispherical Shell of TC4 Titanium Alloy[J]. Rare Metal Materials and Engineering, 2026, 55(07): 1683-1691. DOI: https://doi.org/10.12442/j.issn.1002-185X.20250526.

ARTICLE

Wall Thickness Homogenization Control and Performance of Superplastically Formed Hemispherical Shell of TC4 Titanium Alloy

Ji Wei[1,2], Zhang Zhaohuang[1], Lu Zichuan[3], Wei Shi[3], Qiu Xuyangfan[3], Zhang Xuhu[3]

[1] North China Electric Power University, Beijing 102206, China; [2] China Academy of Aerospace Science and Innovation, Beijing 100076, China; [3] Aerospace Research Institute of Materials and Processing Technology, Beijing 100076, China

Abstract: Spherical and capsule-shaped surface tension tanks are widely used in satellite, spacecraft, and other fields due to their advantages of lightweight structure, high efficiency, and high reliability. With the advancement of space exploration, the demands for thinner walls, more complex structures, and uniform overall performance in the hemispherical shells of these tanks present significant challenges for hemispherical shell forming technique. A hemispherical shell with uniform wall thickness was prepared using the rapid direct-and-reverse superplastic forming method. Results reveal that the properties and microstructure of each section of the formed hemisphere shell are consistent with those of the initial plate, and the overall shell thickness is highly uniform.

Key words: hemispherical shell of storage tank; control of wall thickness; direct-and-reverse superplastic forming; mold design

1 Introduction

The storage tank is a crucial component of the attitude and orbit control system on the satellite platform. It accounts for 80%–90% of the volume and mass of satellite, and it serves as the container of the propellant for orbital transfer and attitude control[1–3]. If the tank fails, the service life of the satellite will be shortened, or, in the worst case, the failure will lead to an explosion that destroys the entire satellite. Due to the critical role of the storage tank, the design and manufacture must ensure maximum strength and load-bearing capacity. Furthermore, the installation and connection to the satellite platform must minimize stress and maximize bearing capacity. However, the restricted capacity of the rocket requires the satellite platform to be as lightweight as possible for carrying as much as possible payload and propellant. These two contradictory requirements compel engineers to select the optimal design.

The tanks used in current satellite platforms can generally be classified into three structural categories: surface tension tank, membrane (membrane box) tank, and capsule tank. Among them, surface tension tanks are solely composed of metallic welded structures without moving parts during operation. This design ensures high reliability, lightweight structure, and excellent expulsion efficiency. Owing to these advantages, surface tension tanks have become the preferred choice for propellant storage in space engineering applications.

Ti-6Al-4V (TC4) alloy, a well-established $\alpha+\beta$ titanium alloy, is widely used for the shells and internal components of surface tension tanks owing to its low density, high strength, high yield-to-tension ratio, broad service temperature range, excellent media compatibility, and superior corrosion resistance[4–7]. With the development of the aerospace industry, the service life and exploration range of satellite platforms and probes have been significantly improved in recent years, resulting in larger tank volumes and imposing significant challenges for the formation of hemispherical shells. For thin-walled hemispherical shells with meter-scale diameters, conventional forging processes impose stringent demands on equipment capabilities. Moreover, the extensive deformation often leads to microstructural inhomogeneity across the shell, resulting in performance variations that may compromise in-

Received date: October 12, 2025
Foundation item: National Natural Science Foundation of China (52203378, 52301143)
Corresponding author: Qiu Xuyangfan, Ph. D., Aerospace Research Institute of Materials and Processing Technology, Beijing 100076, P. R. China, E-mail: 18401669210@163.com

service safety[8].

As a near-net forming technique operating at low strain rates, superplastic forming is widely employed in the aerospace, medicine, and other fields due to its advantages of high forming accuracy, low forming pressure, and high automation in the forming process[9–11]. However, the superplastic forming process is typically conducted at the temperatures near the phase transformation point of titanium alloys, and the process duration is relatively long. During the forming process, the titanium alloy plate undergoes recrystallization and grain growth, which can lead to a slight reduction in the room-temperature mechanical properties of the formed hemisphere shell, compared with those of the original plate[7,12–13].

In addition, during the expansion of the tank shell blank from a flat plate to a hemisphere shape, the increase in superficial area relies entirely on the thickness reduction, following the principle of constant volume. As the forming progresses and the apex of the hemisphere conforms to the mold, the thickness reduction usually differs in different regions of the formed hemisphere shell, and the thickness reduction ratio in the top region can exceed 75%. Such non-uniform deformation introduces significant variations in the mechanical properties across different regions of the hemisphere shell, which may adversely affect the structural reliability of the surface tension storage tank under service conditions[14].

To mitigate the adverse effects associated with superplastic forming of tank shells, this study employed a direct-and-reverse expansion superplastic forming process to fabricate the hemispherical shell. An optimized reverse expansion surface design was implemented to achieve the uniform wall thickness distribution throughout the formed hemisphere shell. Additionally, the forming process was segmented and optimized based on the strain rate sensitivity exponent, effectively reducing the high-temperature forming time. Finally, the formed hemisphere shell was sectioned, and the microstructures and mechanical properties at various locations were analyzed to validate the effectiveness of the process optimization.

2 Experiment

The principal part of the titanium alloy surface tension tank shell consists of large thin-walled hemisphere shells. Certain areas require assembly or welding with other components, necessitating circumferential thickening and reinforcement. As shown in Fig. 1, the main wall thickness of the hemisphere shell is 0.8 mm. At the top region and the region with an angle of 30° to the horizontal axis, the thickness increases to 2 mm for meeting the requirement of the nozzle welding procedure. A ring reinforcement with a thickness of 5 mm was located at the waist region to support the installation of the partition plate. At the horizontal axis (equator), a lock butt structure was adopted, where the wall thickness reached the maximum value of 6 mm.

Considering the subsequent machining and the requirement for uniform wall thickness distribution, the wall thickness of the formed hemispherical shell was designed in the range of 6 – 8 mm. During superplastic forming, when the sheet is transformed from a flat geometry to a hemispherical shape based on the principle of volume conservation, the increase in surface area is entirely accommodated by a reduction in wall thickness. The average wall thickness was 7 mm after forming, and the initial sheet thickness was 14 mm.

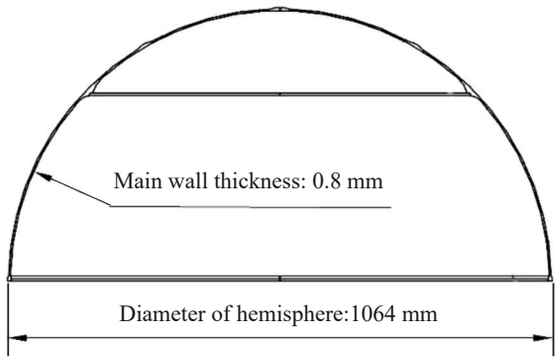

Fig.1 Schematic diagram of hemisphere shell structure of surface tension tank

Thus, the equiaxed fine-grained superplastic TC4 titanium alloy sheet with thickness of 14 mm (produced by Baoti Group) was used to fabricate the hemispherical shell of the surface tension tank. The chemical composition and superplastic properties of the alloy sheet are listed in Table 1 and Table 2, respectively. B and n are material parameters. The specific forming temperature for the TC4 alloy is 900 °C, and the temperature of the phase change point is 990 °C.

In this study, FSP-800 superplastic forming/diffusion bonding equipment (manufactured by ACB, France) was used. The system offered a maximum operating temperature of 1000 °C, a maximum gas-forming pressure of 3.0 MPa, a pressure response time of ≤0.1 s, and a pressure control accuracy of up to 0.0001 MPa. The superplastic forming temperature was set to 900 °C. The forming process of the hemispherical shell was simulated using the finite element software MSC. MARC to obtain an optimized pressure-time curve with the target strain rate controlled at approximately 9.8×10^{-4} s^{-1}. During the diffusion bonding stage, the temperature was maintained at 900 °C under a pressure of 3 MPa for 80 min. The plate was meshed using the quadrilateral

Table 1 Chemical composition of TC4 titanium alloy sheet (wt%)

Al	V	Fe	C	H	O
5.800	4.200	0.020	0.010	0.002	0.120

Table 2 Performance parameters of TC4 titanium alloy sheet

Sheet thickness/mm	Grain size/μm	B	n	Friction coefficient
14	12	1030	0.51	0.16

shell elements. Due to the small rebound after superplastic deformation, which can be ignored in practical engineering applications, a rigid-plastic power-law constitutive model was adopted[15–16], as follows:

$$\sigma_y = B\dot{\varepsilon}^n \quad (1)$$

where σ_y is the yield stress; $\dot{\varepsilon}$ is the equivalent strain rate; B and n are the material parameters. m is the strain rate sensitivity index, and it can be expressed as follows:

$$m = \frac{\mathrm{d}\ln\sigma}{\mathrm{d}\ln\dot{\varepsilon}} \quad (2)$$

where σ is the stress.

To ensure the uniformity of various performance indicators of the spherical shells of surface tension tank during service, this study adopted a direct-and-reverse superplastic forming method for controlling the wall thickness homogeneity. Numerous studies have shown that this technique offers significant advantages in the dimensional accuracy and thickness uniformity of thin-walled complex components. By integrating finite element numerical simulations, the forming outcomes can be accurately predicted and analyzed. Sergey et al[17] investigated the influence of forming processes on the accuracy control of free-forming. Jiao et al[18] concluded that reducing the friction coefficient significantly improves the wall thickness distribution of cylindrical parts fabricated by the direct-and-reverse superplastic forming. However, few analyses have been conducted on wall thickness control in large-sized thin-walled shell components.

Therefore, three influencing factors—the shape of the reverse preforming mold surface, the detailed features of the reverse preforming surface, and the control of forming process parameters—were investigated in this research to optimize the process parameters to achieve uniform wall thickness control in the direct-and-reverse superplastic forming of hemispherical shells.

Tensile tests were performed using the Instron 8801 testing machine at room temperature with a strain rate of 1×10^{-3} s^{-1}. Under each condition, three samples were tested in order to confirm the repeatability of tensile properties. Electron backscatter diffraction (EBSD) measurements were performed at an accelerating voltage of 15 kV and a step size of 0.5 μm. The average grain size was measured by EBSD for the grains with minimum misorientation angles of 15° (excluding the twin boundaries). The tensile loading direction and EBSD sampling positions were aligned along the circumferential direction of the hemisphere.

3 Results and Discussion

3.1 Effects of reverse forming surface design on thickness distribution of hemisphere wall

Fig. 2 shows wall thickness distributions of hemisphere shells prepared by unidirectional and direct-and-reverse expansion superplastic forming methods. As shown in Fig. 2, the finite element simulations display that when the hemispherical shell of a surface tension tank is formed using the unidirectional forming method, the top region is the last region being contact with the mold during forming, and it undergoes the greatest deformation and the most severe thinning deformation.

It can be seen that the simulated thickness of top area of the hemisphere shell is only 4.126 mm, which corresponding to a thinning rate of 70.5%. The wall thickness of the effective portion of the hemisphere shell ranges from 4.150 mm to 9.430 mm with a thickness variation rate of 56.3%. However, in the direct-and-reverse expansion superplastic forming process, reverse preforming can be applied, whereby the local area near the equator region of the hemisphere shell is pre-deformed in the opposite direction. This causes the surface area of this region to increase, and its thickness decreases in advance, as illustrated in Fig.2b.

It is worth noting that the friction coefficient has a significant influence on reverse expansion forming process, which is mainly manifested as the fact that the lower the friction coefficient, the more pronounced the plate sliding during deformation. This phenomenon reduces local stretching and promotes more uniform tensile deformation, ultimately leading to a greater wall thickness variation in the final hemispherical shell[19]. When the friction coefficient is larger, plate sliding becomes more difficult, and the increase in surface area is achieved mainly through local tensile deformation caused by greater external forces. In this case, the thickness of top area retains as that of the initial plate, whereas the thickness of waist region undergoes reduction.

In the direct-expansion process, the increase in surface area will effectively reduce deformation in the top region of the hemisphere shell. Meanwhile, the thinning process at the waist region lowers deformation resistance during subsequent forming process, leading to more pronounced stretching in this region. As a result, thinning at the top area of hemisphere shell is reduced.

After reverse-expansion process, the thickness of top area of the hemisphere shell reaches 7.250 mm, representing a significant improvement over unidirectional forming. However, the waist area is thinned, and the thinnest thickness is 4.760 mm. The wall thickness of the effective section ranges from 4.760 mm to 7.500 mm, resulting in a thickness variation rate of 36.5%. This process changes the overall thickness distribution pattern, which has a considerable adverse impact on subsequent manufacturing, particularly for

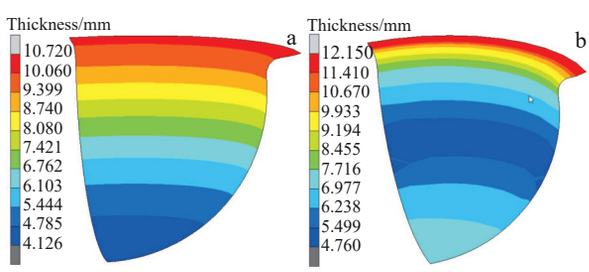

Fig.2 Wall thickness distributions of hemisphere shells prepared by unidirectional (a) and direct-and-reverse expansion superplastic (b) forming methods

the tank structures with ring reinforcements.

To address the above issue, a small amount of reverse-expansion preforming was applied to the top area of the hemisphere shell in this research. For this preforming process, a wave-shaped cross-section mold was adopted. As shown in Fig. 3, the wall thickness of the formed hemisphere shell exhibits a more uniform distribution. Compared with the conventional direct-and-reverse expansion superplastic forming, the proposed method ensures a thickness distribution pattern consistent with that of unidirectional forming, thereby achieving wall thickness homogenization. Fig. 4 shows the simulated wall thickness results. It is demonstrated that the minimum thickness at the top area of the molded hemisphere shell is 5.130 mm, and the thickness of the effective section ranges from 5.230 mm to 7.430 mm, which indicates a further optimization of the homogenization control of thickness.

3.2 Effects of deformation in reverse-expanded area on thickness distribution of hemispherical wall

To further achieve the homogenization control of the wall thickness of the formed hemisphere shell, details of the reverse-expanded surface were analyzed and optimized. The homogenization control of wall thickness in cylindrical components has been conducted through direct-and-reverse expansion superplastic forming[18]. A design method for the reverse-expansion preforming mold surface was proposed, which can significantly reduce wall thickness variation after forming[18]. However, the direct-and-reverse expansion superplastic forming method used for the large-size surface tension tank of titanium alloy has been rarely studied. Therefore, building upon this approach and considering the structural characteristics of hemispherical propellant tank shells, three key variables of the reverse forming die profile—center preforming height (h), center preforming radius (d), and equator preforming height (H) —are analyzed, as shown in Fig. 5. The effects of these parameters on the wall thickness distribution of the hemisphere shell are investigated, and an appropriate process design scheme is proposed.

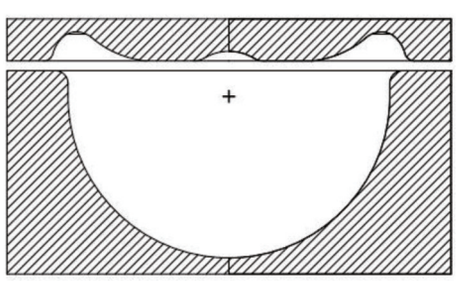

Fig.3 Schematic diagram of mold for homogeneity control in direct-and-reverse expansion superplastic forming

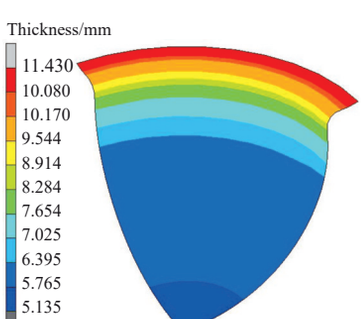

Fig.4 Wall thickness distribution after direct-and-reverse expansion superplastic forming

Firstly, the effects of the center preforming height h at the hemisphere top region on the wall thickness distribution after forming were investigated. Models were established under the conditions of h=30, 45, and 60 mm, d=90 mm, as well as H=90 mm. Finite element simulation results indicate that with the increase in reverse preforming height h, the wall thickness of the hemisphere top area is continuously decreased. In this research, T_{min} and T_{max} represent the minimum and maximum effective thickness of the hemisphere shell, respectively. As shown in Fig. 6, comparing the effective region of the hemisphere shell, it can be seen that the wall thickness at the equator region barely changes with the increase in h value. However, in the top region, a higher h value during preforming increases the deformation amount and the degree of pre-thinning. In the subsequent forming process, the reduced thickness in the top region lowers its deformation resistance, causing further tensile deformation as the sheet comes into contact with the mold. This results in a greater variation in wall thickness distribution after forming. Therefore, h=30 mm is selected as the optimal parameter value for subsequent analysis.

Secondly, the effect of the center preforming radius d on the wall thickness of the formed hemisphere shell was analyzed under the conditions of h=30 mm, d=90, 120, 150, and 180 mm, as well as H=90 mm. Finite element simulation results are shown in Fig. 7. With the increase in d value, the wall thickness distribution of the hemisphere shell becomes more uniform, and the thickness of top region is increased slightly. When d increases from 90 mm to 120 mm, the thickness of top region rises from 5.230 mm to 5.480 mm. However, further increasing d value to 180 mm results in only a minor thickness increase from 5.480 mm to 5.580 mm. The increment is only 0.100 mm, which is negligible for engineering applications. Therefore, d=120 mm is selected as the optimal parameter value for subsequent analysis.

Thirdly, the effect of the equator preforming height H on the wall thickness of the formed hemisphere shell was analyzed under the conditions of h=30 mm, d=120 mm, as well as H=90, 105, and 120 mm. Finite element simulation results are shown in Fig. 8. When H value increases from 90

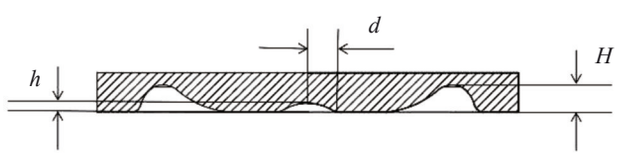

Fig.5 Schematic diagram of mold parameters of direct-and-reverse expansion preforming

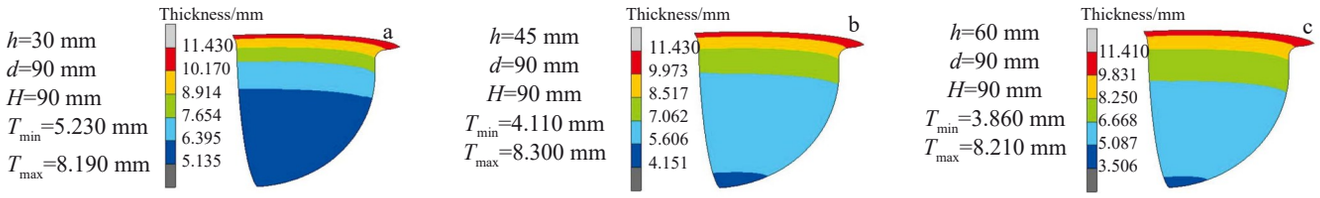

Fig.6 Effects of center preforming height *h* on wall thickness of hemisphere shell: (a) *h*=30 mm; (b) *h*=45 mm; (c) *h*=60 mm

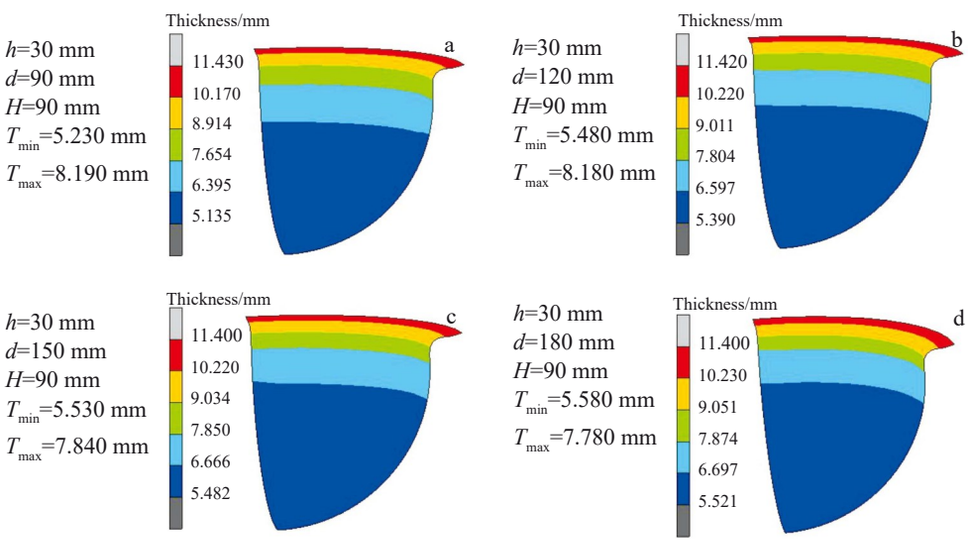

Fig.7 Effects of center preforming radius *d* on wall thickness of hemisphere shell: (a) *d*=90 mm; (b) *d*=120 mm; (c) *d*=150 mm; (d) *d*=180 mm

mm to 105 mm, the thickness of the top region is increased slightly from 5.480 mm to 5.520 mm, whereas the thickness of equator region is decreased from 8.180 mm to 7.920 mm, indicating minimal overall change. However, when *H* value further increases to 120 mm, the thickness distribution changes notably, exhibiting a thin-thick-thin-thick pattern from the top to the equator region. At this point, the thickness of top region reaches 6.350 mm, which is a remarkable increase compared with that under *H*=90 and 105 mm. Nevertheless, the thinnest region shifts to the waist part, whose the thickness drops to only 5.250 mm, thus failing to achieve effective homogenization control of the wall thickness of the hemisphere shell.

Based on the above numerical simulations, the parameters *h*=30 mm, *d*=120 mm, and *H*=105 mm are selected as the optimal parameters. Simultaneously, the curvature and fillet radius of the mold surface are also further optimized, leading to the final forming surface design and mold fabrication. To ensure full conformity of the hemispherical shell with the mold in the final contact region, five vent holes were arranged in a ring pattern: one at the pole, and four evenly spaced along the polar circle. As shown in Fig. 9, finite element analysis of the optimized surface indicates that the wall thickness in the effective region of the hemisphere shell ranges from 6.080 mm to 7.430 mm with a variation rate of only 18.2%. The wall thickness distribution map exhibits that from the top region to the region with radius of 400 mm, the thickness of the hemisphere shell barely changes, exhibiting a thin-thick-thin pattern between 6.080–6.450 mm. From the region with radius of 400 mm to the equator region, the thickness increases linearly from 6.080 mm to 7.430 mm. The increase in wall thickness is beneficial to the subsequent design of reinforcement by electron beam welding in the equator region.

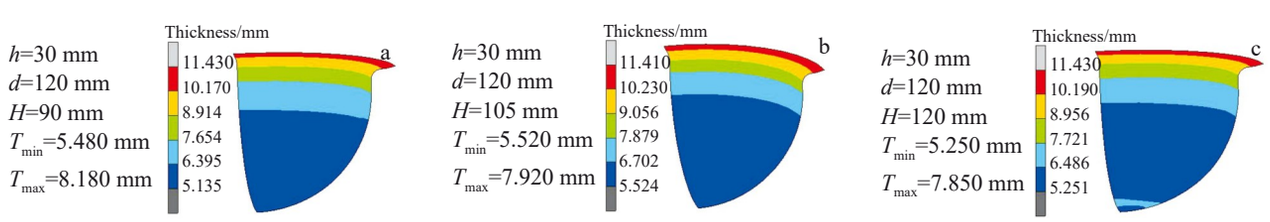

Fig.8 Effects of equator preforming height *H* on wall thickness of hemisphere shell: (a) *H*=90 mm; (b) *H*=105 mm; (c) *H*=120 mm

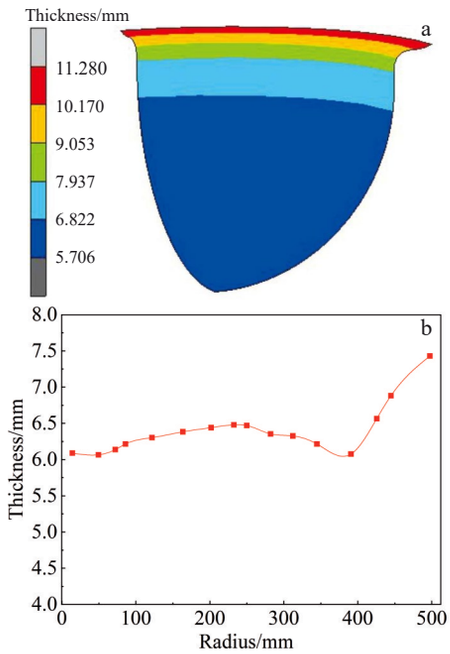

Fig.9 Wall thickness distribution map (a) and profile (b) of hemisphere shell prepared with optimized parameters

3.3 Simulation of pressure-time relationship

The reverse-and-direct expansion superplastic forming processes were separately defined as load cases. For the reverse forming process, the strain rate was set to 0.001 s^{-1} with the duration of 1100 s and a maximum pressure of 3.0 MPa. For the direct-expansion forming process, the strain rate was set to 0.0005 s^{-1} with the duration of 2000 s and a maximum pressure of 1.5 MPa. The time-pressure curves at constant strain rates are fitted using Marc numerical simulation software, and the results are shown in Fig. 10. In the reverse-expansion forming process, the pressure increases almost linearly to 3.0 MPa and retains until the end of the process. In the direct expansion forming process, the pressure is increased linearly to 0.90 MPa, held at 0.90 MPa for 600 s, and then gradually reduced to 0.70 MPa. Finally, after forming, the pressure rises to 1.5 MPa and retains to ensure full contact between the hemispherical shell and the mold, preventing rebound.

3.4 Forming results and structure performance analysis

To investigate the influence mechanism of superplastic forming process on the overall microstructure evolution and mechanical properties of the storage tank shell, and to evaluate the service performance of the final shell, cross section of the formed hemisphere shell was analyzed. Because the wall thickness distribution of the hemisphere shell produced by direct-and-reverse expansion superplastic forming is generally uniform, samples were taken from different height zones for comparative analysis.

Fig.11 presents the results of the mechanical property test at room temperature of the raw materials and formed hemisphere shell. It can be seen that the raw material (TC4 alloy) exhibits excellent mechanical properties at room temperature. After

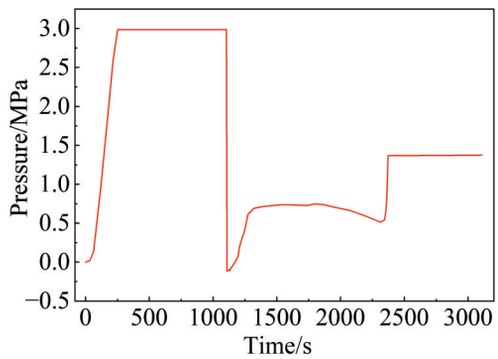

Fig.10 Simulated pressure-time curve of hemisphere shell during reverse-and-direct expansion superplastic forming process

direct-and-reverse expansion superplastic forming, the tensile strength at different heights of the hemisphere shell is basically about 1000 MPa, which is slightly lower than that of the raw material by approximately 50 MPa. The elongation increases significantly from 16% (raw material) to 20%, indicating a substantial plasticity reserve and an excellent strength-ductility balance.

Fig. 12 shows EBSD maps with grain boundary distribution of raw material and different regions of hemisphere shell, where red, green, and blue lines represent low-angle boundaries ($2°<\theta<5°$), medium-angle boundaries ($5°<\theta<15°$), and high-angle boundaries ($\theta>15°$), respectively. As shown in Fig. 12a, the raw material exhibits a typical $\alpha+\beta$ type bimodal equiaxed recrystallized structure with an average grain size of 12 μm, ensuring excellent superplastic forming capacity. According to Fig. 12b – 12d, the microstructure of the hemisphere shell does not differ significantly from that of the raw plate, still presenting a typical bimodal equiaxed fine-grained $\alpha+\beta$ structure. However, smaller equiaxed α phases can be observed, and they are enriched around locally larger equiaxed primary α phases. The distributions of low-angle boundary, medium-angle boundary, and high-angle boundary show slight variations.

According to Ref.[20], the superplastic forming process is a thermal deformation process, during which the work-hardening regions within the raw material (characterized by dislocation entanglements and typically represented by low-

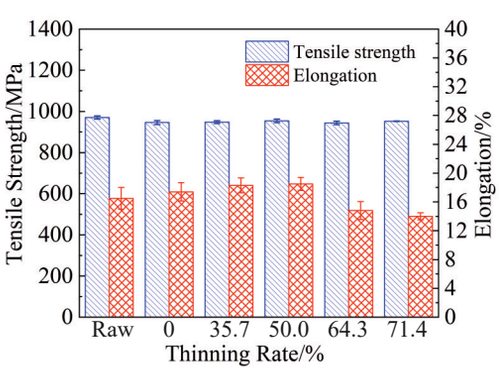

Fig.11 Mechanical properties of raw material and different regions of hemisphere shell

angle boundaries) undergo dislocation glide and climb under the action of thermal driving forces. This process leads to the formation of dislocation substructures, which gradually evolve into equiaxed fine dynamically-recrystallized grains. Therefore, the superplastic forming process inherently exerts a grain-refining effect[21].

In addition, compared with the raw material, Fig. 12b–12d clearly show the presence of medium-angle boundaries (marked by green line) within the large primary α grains. This is attributed to the fact that substructure features, such as dislocation walls formed during the thermal deformation process, are not transformed into high-angle boundaries and thus remain within the grain as transitional defects during dynamic recrystallization. Consequently, the dynamic recrystallization during superplastic forming process effectively refines the grains, enhances grain-to-grain deformation compatibility, and reduces local stress concentration factors, thus improving the elongation after forming[22]. However, since dynamic recrystallization also reduces the strain hardening capacity in the raw material, the tensile strength of the formed shell is slightly lower than that of the raw material.

Fig. 13 shows EBSD phase maps of raw material and different regions of hemisphere shell. It can be seen that the β phase, as an intercrystalline phase, is evenly distributed around the α phase in the raw material with the volume fraction of approximately 2.6%. After forming, the β phase accounts for approximately 7.9%–10.0% at different regions. The β phase, as a soft intercrystalline phase with a body-centered cubic crystal structure remains evenly distributed around the α phase grains of the hexagonal close-packed crystal structure, acting as an effective grain boundary lubricant during deformation and contributing to the grain boundary accommodation[23].

Fig. 14 presents the inverse pole figures (IPFs) of raw material and different regions of hemisphere shell. The grains of different colors correspond to different grain orientations. Since the raw material in this study was annealed, the

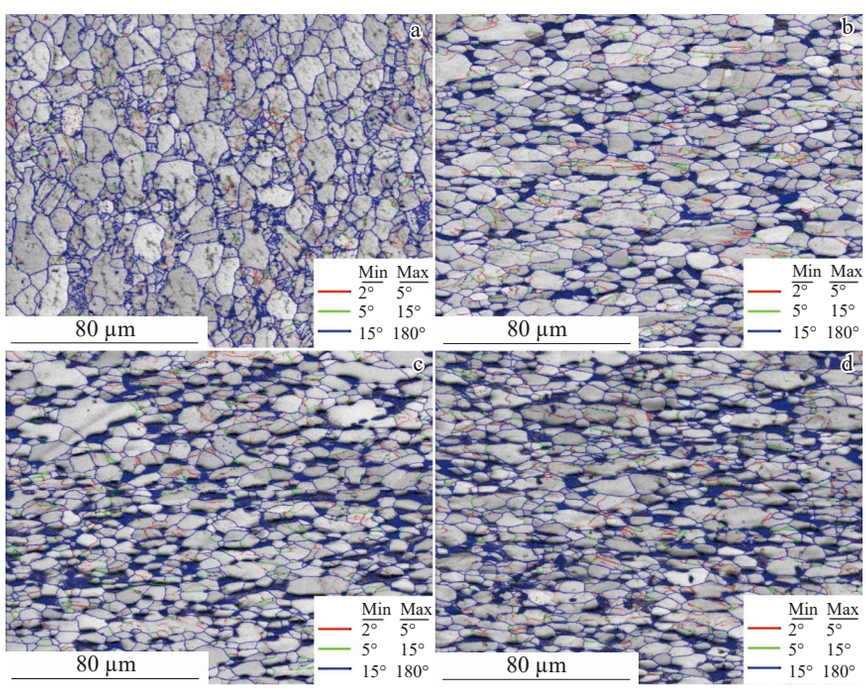

Fig.12 EBSD maps of raw material (a) and different regions of hemisphere shell (b–d): (b) thinning rate of 35.7%, (c) thinning rate of 50.0%, and (d) thinning rate of 64.3%

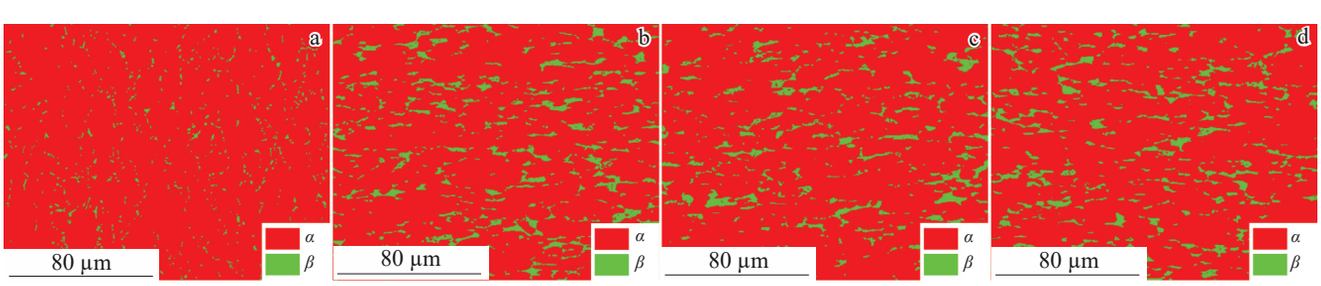

Fig.13 EBSD phase maps of raw material (a) and different regions of hemisphere shell (b–d): (b) thinning rate of 35.7%, (c) thinning rate of 50.0%, and (d) thinning rate of 64.3%

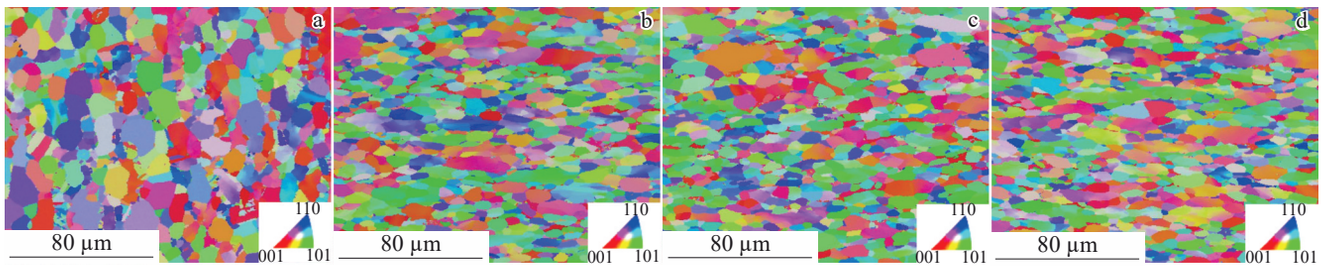

Fig.14 IPFs of raw material (a) and different regions of hemisphere shell (b–d): (b) thinning rate of 35.7%, (c) thinning rate of 50.0%, and (d) thinning rate of 64.3%

distributions of grain size and grain orientation are relatively uniform, and the grains exhibit non-pronounced preferred orientation. The strong rolling texture is effectively eliminated, ensuring uniform isotropic deformation during the direct-and-reverse expansion superplastic forming process. Fig. 14b – 14d indicate that the primary α phase and newly formed fine dynamic recrystallization grains maintain a statistically random crystallographic orientation, which is highly favorable for isotropic uniformity of the tank shell during the pressurization. This is a key factor to ensure the excellent service performance of pressure vessels.

The above mechanical properties and microstructure analyses demonstrate that the tank shell produced by the direct-and-reverse expansion superplastic forming process exhibits excellent strength-ductility balance and performance. Furthermore, the overall microstructure and phase components are uniform and consistent, and the crystallographic orientations are randomly distributed without any pronounced texture, ensuring uniform pressure-bearing capacity of the hemisphere shell and enhancing its service performance.

Based on the simulated pressure-time curve, the forming process parameters are optimized in combination with the equipment capability, and the optimized curve is shown in Fig.15. It can be seen that the optimized forming parameters result in slower pressure increase. However, the durations of the forming-pressure stage and pressure-holding stage are consistent with the simulated results, and the total duration is

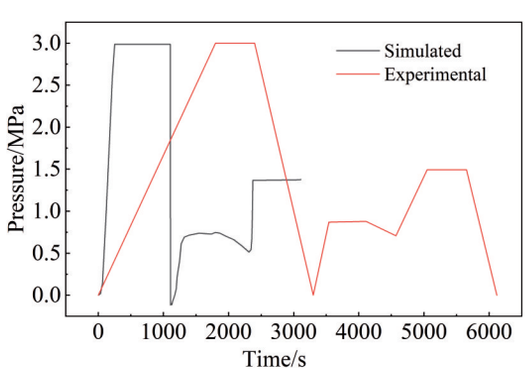

Fig.15 Simulated and experimental pressure-time curves of hemisphere shell during reverse-and-direct expansion superplastic forming process

6120 s. Based on the fitted pressure-time curve of the forming process, the forming time is minimized as much as possible while ensuring both the surface precision of the hemispherical shell and compatibility with the equipment capacity.

The appearance of the final hemisphere shell is shown in Fig. 16. After direct-and-reverse superplastic forming, the hemisphere shell was treated by electron beam welding, yielding a surface tension tank that meets both dimension and precision specifications. This tank can bear cyclic pressure of 5 MPa, which can be applied in the spacecraft applications.

Fig.16 Appearance of surface tension tank for propellant storage

4 Conclusions

1) Based on the fitted pressure-time curve of the forming process, the forming time is minimized as much as possible while ensuring both the surface precision of the hemispherical shell and compatibility with the equipment capacity. The performance across different regions of hemisphere shell is essentially consistent. The tensile strength at different regions of the hemisphere shell is basically about 1000 MPa, which is slightly lower than that of the raw material by approximately 50 MPa, Besides, the elongation is notably improved.

2) The dynamic recrystallization during superplastic forming process, which effectively increases the number of fine recrystallized grains, enhances intergranular deformation compatibility and reduces local stress concentration.

Moreover, the crystallographic random orientation retains, which is beneficial to the uniform stress distribution during the service of the tank shell.

References

1 Hsieha S C, Chenb J H, Leea A C. *Journal of Sound Vibration* [J], 2008, 289(1): 294

2 Ede Z Q, Howe D. *IEEE Transactions on Industry Applications* [J], 2022, 38(6): 1542

3 Jiang Shaosong, Zhang Kaifeng, Wu Haifeng *et al*. *Rare Metal Materials and Engineering*[J], 2010, 39(6): 1079 (in Chinese)

4 Yoon J H, Lee H S, Yi Y M. *Journal of Materials Processing Technology*[J], 2008, 201(1–3): 68

5 Odenberger E L, Oldenburg M, Thilderkvist P *et al*. *Journal of Materials Processing Technology*[J], 2011, 211(8): 1324

6 Sun Z C, Yang H, Han G J *et al*. *Materials Science and Engineering A*[J], 2010, 527(15): 3464

7 Tersing H, Lorentzon J, Francois A *et al*. *Finite Elements in Analysis & Design*[J], 2012, 51(2): 10

8 Li Changliang, Zhao Yongqing, Ding Hua *et al*. *Rare Metal Materials and Engineering*[J], 2002, 31(6): 476 (in Chinese)

9 Pei Chuanhu, Li Zhenxi, Ding Jianshan *et al*. *Rare Metal Materials and Engineering*[J], 2017, 46(S1): 118 (in Chinese)

10 Wang Min, Lin Chengxiao. *Rare Metal Materials and Engineering*[J], 2012, 41(7): 1176 (in Chinese)

11 Xu Xuefeng, Wang Gaochao, Xia Chunlin. *Rare Metal Materials and Engineering*[J], 2012, 41(3): 527 (in Chinese)

12 Velay V, Matsumoto H, Vidal V *et al*. *International Journal of Mechanical Sciences*[J], 2016, 108–109: 13

13 Zhang T, Liu Y, Sanders D G *et al*. *Materials Science and Engineering A*[J], 2014, 608(1): 265

14 Liu G, Wu Y, Zhao J *et al*. *Procedia Engineering*[J], 2014, 81: 2243

15 Chumachenko E N. *Materials Science and Engineering A*[J], 2009, 499(1–2): 342

16 Fan X G, Yang H, Gao P F. *Materials & Design*[J], 2013, 51: 34

17 Sergey A V K, Aksenov A, Anastasia V. *Journal of Materials Processing Technology*[J], 2010, 237: 88

18 Jiao F P, Fu Z D, Li S *et al*. *Trans Nonferrous Met Soc*[J], 2012, 22(2): 476

19 Balasubramanian M, Ramanathan K, Kumar V S S. *Procedia Engineering*[J], 2013, 64: 1209

20 Shen J, Sun Y, Ning Y *et al*. *Materials Characterization*[J], 2019, 153: 304

21 Huang L J, Lu S, Yuan L *et al*. *Materials & Design*[J], 2016, 93(3): 81

22 Kim J S, Kim J H, Lee Y T *et al*. *Materials Science and Engineering A*[J], 1999, 263(2): 272

23 Zhang T, Liu Y, Sanders D G *et al*. *Materials Science and Engineering A*[J], 2014, 608(6): 265

TC4钛合金超塑性半球形壳体壁厚均匀化控制及性能

纪　玮[1,2]，张照煌[1]，陆子川[3]，微　石[3]，邱旭扬帆[3]，张绪虎[3]

(1. 华北电力大学，北京 102206)

(2. 中国航天科技创新研究院，北京 100076)

(3. 航天材料及工艺研究所，北京 100076)

摘　要：球形/胶囊形表面张力贮箱以其结构轻、效率高、可靠性高等优势，在卫星、航天器等领域得到广泛应用。随着航天事业的发展，表面张力贮箱的半球壳体主体壁厚进一步减薄、结构更为复杂、整体性能一致等要求对半球成型工艺带来极大挑战。采用快速正反向超塑成型法，通过调整反向预成型型面，成功实现半球整体壁厚均匀化成型。结果表明，成型后的半球壳体各部位性能、组织形态与初始板材基本一致，半球壳体壁厚具有良好均匀性。

关键词：贮箱半球形外壳；壁厚控制；正反向超塑性成型；模具设计

作者简介：纪 玮，男，1985年生，博士，高级工程师，华北电力大学，北京 102206，电话：010-68795828，E-mail：13911102596@163.com